

Powerful Nanosecond Single-Shot Technique for Detection of Illicit Materials and Explosives

V.A. Gribkov 1), S.V. Latyshev 1), R. Miklaszewski 2), M. Chernyshova 2),
K. Drozdowicz 3), U. Wiącek 3), A.V. Dubrovsky 4), B.D. Lemeshko 4)

- 1) A.I. Alikhanov Institute for Theoretical and Experimental Physics (ITEP), Moscow, Russia
- 2) Institute of Plasma Physics and Laser Microfusion (IPPLM), Warsaw, Poland
- 3) Institute of Nuclear Physics (INP), Krakow, Poland
- 4) N.L. Dukhov All-Russia Research Institute of Automatics (VNIIA), Moscow, Russia

Email contact of main author: gribkovv@yahoo.com

Keywords: Detection, Fast neutrons, Explosives

Abstract. Recent progress in a single-pulse nanosecond technique of interrogation of unknown (hidden) objects by means of measuring of the elastically scattered neutrons is presented. The method uses very bright neutron pulses having duration of the order of 10 ns generated by Dense Plasma Focus (DPF) devices. Small size occupied by the neutron flash in space, its intensity and mono-chromaticity ($\Delta E/E \sim$ a percent) ensure an opportunity to use a time-of-flight (TOF) technique with flying bases of about a few meters. In our researches we used a DPF chamber meant for the DPF bank energy of about 5-10 kJ and generating neutron yield on the level of $3 \times 10^8 \dots 10^9$ D-D neutrons per pulse with pulse duration of 15 ns. TOF base in those tests was 18.5 meters. We have demonstrated a possibility in principle the registration of scattered neutrons by the substance under interrogation – ethanol. Here we present an accurate calculation and interpretation of the results obtained for methanol. In the new set of experiments presented also in this report we have experienced an opportunity to use much lower bank energy (~ 2 -3 kJ), smaller DPF chamber, and decreased neutron yield ($\sim 10^8$ n/shot) what results in much lower activation of objects under interrogation and in shorter TOF base as well (2.2 meters). In this case it appears that the neutron pulse duration becomes 7-8 ns whereas the above-mentioned short new TOF base is enough to distinguish different elements' nuclei composing the substance under interrogation (phosphoric acid). We will present also experimental data on use 14-MeV neutrons in this technique (generated by DPF working with D-T gas mixture) as well as some results on neutron irradiation of fission materials. The wavelet technique was engaged to “clean” the experimental data registered.

1. Introduction

The terrorists' attacks on civil objects throughout the world are well known. Traffic of explosives by vehicles on the ground, by sea and air is of an earnest concern. These facts demand elaboration of fast and efficient methods of screening suspicious objects. Methods using fast neutrons may give the necessary solution [1]. They use different sources of penetrating radiations. Between their problems the most important ones are *a high level of dose* needed for identification of materials (current neutron-based technologies require a total flux of $10^{10} \dots 10^{13}$ neutrons per interrogation) and *a low signal-to-noise ratio at the detection part* of the systems (see e.g. [1–3]). Both problems result in a necessity to produce many shots with the generator-based neutron sources ($\sim 10^6 \dots 10^8$ pulses) and in a long interrogation time.

Our method [4, 5] belongs to the wider group of approaches [1] that makes use an interaction of fast neutrons with different materials. As a result of such interaction a field of scattered neutrons is formed. The field appears because of elastic and inelastic scattering of primary neutrons by nuclei of the irradiated matter. Besides an induced gamma radiation is emitted from an object under irradiation. Information on elemental composition of the object can be obtained from spectrum of both the gamma radiation and the scattered neutron field.

Compared with the so-called Fast Neutron Scattering Analysis (FNSA) developed lately by Buffler et al. [2] we proposed [4] to bring into play a neutron source based on a *plasma accelerator* of the Dense Plasma Focus type (DPF). It generates *nanosecond* (ns) pulses of hard X-Rays (HXR) and neutrons having *simultaneously* a *very high intensity* – up to $10^8 \dots 10^{12}$ neutrons and 10...100 J of HXR – per a single pulse. These characteristics open new opportunities for explosives' detection allowing utilization the well-known concept of neutron TOF measurements and HXR object's imaging here just in a single shot of the device.

2. Equipment

We use PF-10 (ITEP, RF, 10-kJ, deuterium, 3×10^8 n/pulse), PF-6 (IPPLM, Poland, 7.4 kJ, deuterium, 10^9 n/pulse) and ING-103 (VNIIA, RF, 3...10 kJ, deuterium-tritium, $10^{10} \dots 10^{11}$ n/pulse) (see Fig. 1). Pulse duration is about 10-ns. These two prerequisites give a principal possibility to create a *single-shot* “Nanosecond Impulse Neutron Investigation System” (NINIS) intended for an interrogation of hidden objects. All main data can be gained by means of the time-of-flight technique with a short flight base. We believe that this method will ensure a profound decrease of signal/noise ratio, a minimization of the overall irradiation dose by 2...3 orders and the interrogation time by 8-9 orders of magnitude compared with existing techniques. It will result in a lower activation of items under inspection and in a decrease of a false alarm rate. Our technique was tested at the neutron yield per a single shot equal to 10^{11} n/shot for D-T mixture as a working gas and 10^9 down to $1 \dots 3 \times 10^8$ n/shot for deuterium.

The DPF-based neutron source is ecologically more acceptable compared with others because it produces a neutron radiation only “on demand” for a few nanoseconds (a so-called “push-button device”) and it doesn't require a special storage as the isotope-based sources. And it uses charging voltage of about 10 kV. This modern DPF is characterized by operation with vacuum-tight (welded) chambers with the life-time of the order of 10^6 “shots”. It has relatively low size and weight (0.5...1.0-m² footprint and 100-400 kg thus it is a transportable device), comparatively low cost, and it obeys a possibility to work with a high repetition rate (tested up to 15 cps), etc. For registration of direct and scattered neutrons as well as hard X-Rays we used PMT+S: Hamamatsu-1949-51 module, S/N WA5952, FWHM = 3.12 ns at the IPPLM and a PMT of the type SNFT with FWHM = 2.5 ns at ITEP and VNIIA.

3. The method

Main principle of the technique used is based on the change of the energy of scattered neutrons, when their energy *dissimilar* decreases due to *elastic* scattering on nuclei of various elements having *different* masses. It must be reflected in a difference of TOF of these neutrons. Element's content (chemical formula) of the interrogated substance can be determined afterwards taking into consideration these time lags, the amplitudes of the neutron pulses scattered by corresponding element's nuclei and the respective cross-sections of the elastic scattering of neutrons on the nuclei of the particular elements.

Scattering signatures of different elements common for explosives (especially nuclei of H, C, N and O, as well as P and some others) should be precisely determined beforehand. Then the data base created will unveil the elemental composition of unknown samples by analysis of their scattering signatures.

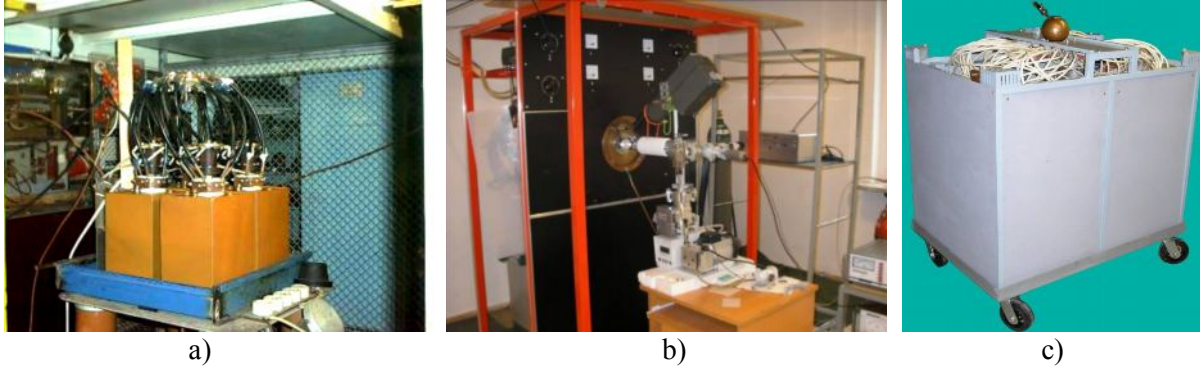


FIG. 1. DPF-10 device (ITEP)(a); PF-6 device (IPPLM) (b) and ING-103 (VNIIA) (c)

Preparatory to provide experimental works we took a number of numerical simulations using the MCNP code to imitate the conditions of our proposed irradiation sessions. The results of these simulations will be presented by Dr. R. Miklaszewski in a separate report. Here we shall mention only two important results of these calculations: 1) We made a proper choice for geometry and distances of our scattering experiments; 2) We found that the number of scattered neutrons at our best geometries is enough to be registered by our technique in both cases – lower-energy neutrons elastically scattered by stable isotopes of C, N, O, and H, and higher-energy neutrons inelastically scattered by fissile materials.

3. Experiments

In all experimental sessions we investigated scattering of neutrons by 1-liter bottles of methanol (CH_3OH), phosphoric acid (H_2PO_4) and nitrogen acid (HNO_3) positioned in a very close vicinity to the DPF chamber. The geometry of the experiments is shown in Fig. 2. In the first case we operate with DPF bank energy on the level of about 7 kJ with neutron output of the device $\sim 10^9$ neutrons per pulse. Our scintillator used for the PMT probe had a diameter 10 cm with its length of 10 cm. A typical result received with them is presented in Fig. 3. The right trace is taken with the higher sensitivity of the oscilloscope. Calculations of neutrons' energy of the first pulse ("n", seen in Fig. 3(b), by using time-of-flight (TOF) data with the help of formula: $E [\text{MeV}] = (L[\text{m}] / t [\text{ns}])^2 \times 5.23 \cdot 10^3$, have shown that their medial energy is ≈ 2.6 MeV. This value is a typical one for neutrons generated in a DPF in forward direction, i.e. within the small angle around Z-axis of its chamber ("head-on" neutrons) [5].

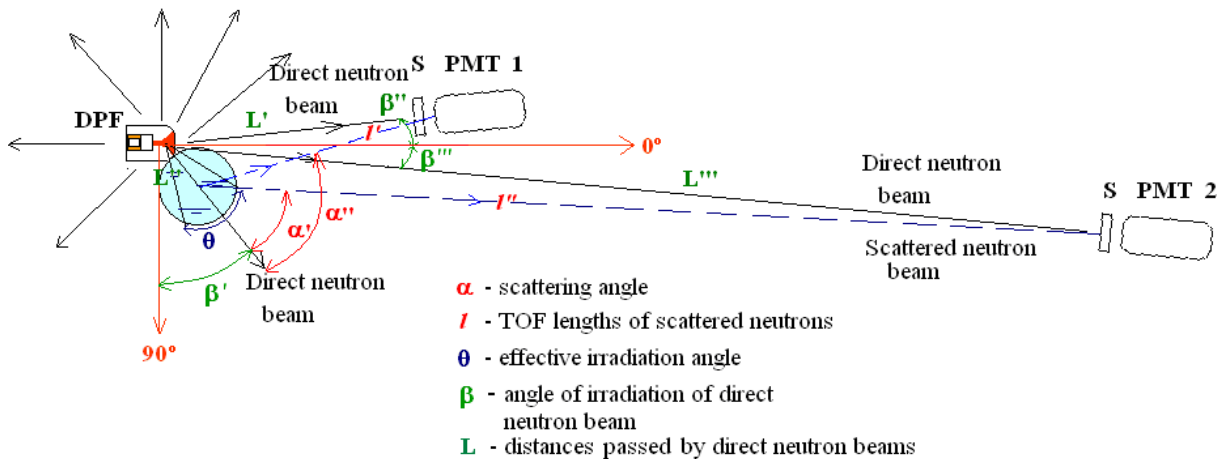


FIG. 2. Scheme of the experiments

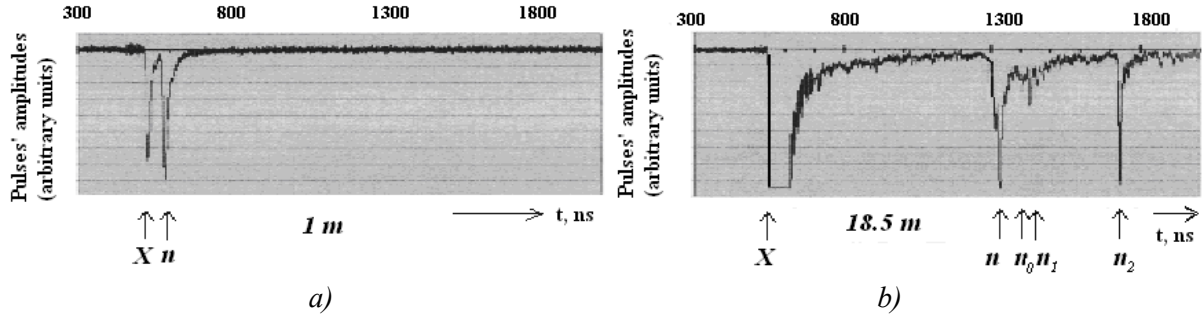


FIG. 3. Oscilloscope traces of PMTs placed at 1.0 (a) and 18.5 meters (b) from the target

However the so-called “side-on” neutrons generated at the angle 90° to Z-axis of a DPF chamber have energy 2.45 MeV. Now we have to understand what would be the energy of the second and the third neutron pulses (“ n_0 ” and “ n_1 ”). To calculate the real position of the above “ n_0 ” and “ n_1 ” neutron pulses on the oscilloscope trace and consequently their TOF and energy we have to perform the following procedures:

- 1) To move *forward* in time (to the left) the hard X-Ray pulse by its TOF of 18.5 m (62 ns) – this will be the moment of the appearance of the front of HXR pulse inside the chamber.
- 2) To move *backward* (to the right) the above point by 8 ns – this will be the moment for neutrons to top out their maximum inside the DPF chamber.

After the above procedure we shall have the *reference point* (“0 ns”), from which we can calculate all time intervals. Taking into consideration that our target is placed at a distance of 20 cm to the DPF chamber’ centre and in the “side-on” position, we have to perform all calculations for the neutrons *having energy 2.45 MeV* and in the conditions that their direct TOF from the centre of the DPF chamber till the target (centre of the bottle) is 10 ns. Effective angle of the bottle’s irradiation was $\theta \approx 10^\circ$. Kinematics of elastic scattering of neutrons by different nuclei is shown in Fig. 4. Our PMT+S probe was placed at the angle α of about 80° to the direction of the neutron beam passing through the centre of the bottle with methanol.

From the graphs based on kinematics of scattering and on our experimental geometry one can see that our two peaks on the oscilloscope trace – “ n_0 ” (908 - 10 = 898 ns) and “ n_1 ” (925 - 10 = 915 ns) – may be attributed to the scattering of the *2.45-MeV neutrons* on the oxygen and carbon nuclei accordingly. For the pulse “ n_2 ” we have analyzed several different possible scatterers (elements in the vicinity of the DPF) and eventually we have found that it is our high-pressure 20-l cylinder with deuterium placed at 1 m from the DPF chamber.

It is interesting to compare cross-sections of 2.45-MeV neutrons, elastically scattered on the above materials, and of 2.6-MeV neutrons – on a 20-cm Teflon cylinder (positioned in the direction of the PMT+S and blocking the “direct” beam of neutrons – see Fig. 1 (b)). It appears that these figures are equal to $\sigma = 3$ barn for the deuterium nuclei, 1.5 barn – for nuclei of ^{12}C , whereas the related magnitude for ^{16}O in this range of $\sigma(E)$ going to a minimum at 2.35 (relatively narrow) is equal to 0.6 barn at its slope. For fluorine and 2.6-MeV neutrons it is on the level of 1.5 barns. These figures together with the geometrical factors (the volumes of our objects) are fitted to the relative ratio for the amplitudes of the peaks “ n ”, “ n_0 ”, “ n_1 ”, and “ n_2 ”.

Our next experiment was devoted to the phosphoric acid (H_3PO_4) used as a target. It was installed tightly with the DPF chamber as it is shown in Fig. 2 with the geometry as follows: $\beta' \approx 35^\circ$, $\beta'' \approx \beta''' \approx 27^\circ$, $L' = 2.2$ m, $L'' = 8$ cm, $\theta \approx 10^\circ$, $L''' = 7$ m. In these tests we have experienced an opportunity to use much lower bank energy (~ 3 kJ).

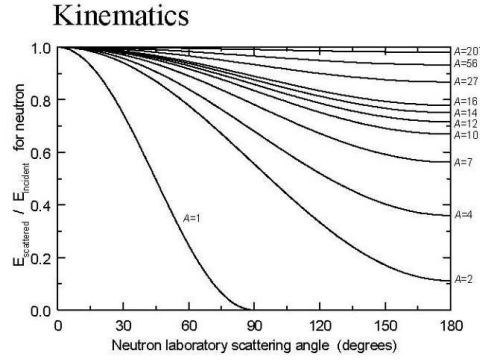


FIG. 4. Graph showing the ratio of energy of neutrons scattered by nuclei of various elements to the initial energy of neutrons of the irradiating beam in dependence of scattering angle

It gave us smaller DPF chamber and decreased neutron yield ($\sim 1 \dots 3 \times 10^8$ n/shot) what results in lower activation of objects under interrogation and in shorter TOF base (2.2 meters). We used here 2 PMT of the SNFT type (2.5 ns time resolution) placed in two different distances from the scatterer – 2.2 and 7 meters. In this case the neutron pulse duration detected at a close vicinity to the DPF chamber became 5-8 ns. Thus the thickness of an almost spherical neutron “shell” spreading from the source is ~ 10 -15 cm.

Two typical oscilloscope traces taken at the experiments with a bottle of phosphoric acid obtained from S+PMT-1 are shown in Fig. 5. These traces were received accordingly for two different situations – when direct neutron beam to the PMT-1 from the DPF chamber was almost completely blocked by a screen (a) and conversely without the screen (b). In Fig. 5 (c) we plot time delays between X-Ray pulse and a pulse of direct neutrons received by two PMT for the above-mentioned distances. Calculations show that for the experiment of Fig. 5 (a) we had a time-delay between the X-Ray front and the neutron maximum equal to 6 ns whereas for Fig. 5 (b) this value was 13.5 ns. These figures were quite important for correct calculation of time intervals for delayed neutrons scattered by a target in an every particular shot.

For calculations of the expected points on the oscilloscope traces where we have to find a peak of direct neutrons (1) we used data received from Fig. 5 (c) (i.e. two values – energy of neutrons at their energy distribution maximum and the delay of its pulse maximum compared to the X-Ray front). As for the neutrons scattered by our target (peaks 2 and 3) we used the procedure described above and in [4], namely we took into consideration the following data:

- 1) Average energy of neutrons E_0' irradiating the target (2.55 MeV) and energy of neutrons directly arrived to the scintillator from the DPF chamber E_0'' (2.70 MeV)
- 2) Angle of irradiation of the target (β'), angle of direct beams propagation to the S PMT (β'' and β''') (for both S+PMT they were the same) and angle of beam of scattered neutrons (α)
- 3) Distances from the source to the axis of the bottle (target) (0.08 m) and from the target centre to the scintillator of PMT (2.2 m)
- 4) Effective irradiation angle of the target for our geometry (θ), and
- 5) Time delay of neutron maximum in relation to the front of hard X-Rays *inside* the DPF chamber (6 and 13.5 ns for Fig. 13 and 14 respectively).

The neutron detector signals contain an essential noise component in this our case of low dose of neutrons. Trying to de-noise these signals, we used wavelet method suggested by MATLAB Wavelet Toolbox. We used De-noising 1-D. We considered the noise to be un-scaled white. The signal was presented by 2048 numerical points.

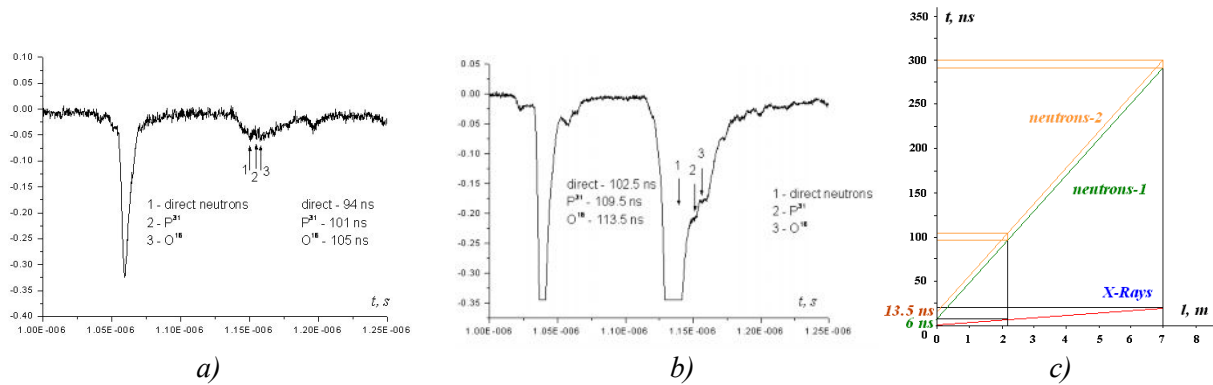


FIG. 5. Oscilloscope traces with direct beam of neutrons (1) blocked almost completely by a neutron screen (a) and without shielding (b) and TOF of X-Ray and neutron pulses at 2.2 and 7.0 meters (c)

We used soft fixed form of the threshold method. Fig. 6 (a) and (b) show the above two oscilloscope traces, where the “dmey” wavelet was used in both cases at the level 2. One can see that the results of the wavelet de-noising allow identifying reliably peaks 1, 2, and 3.

After elastic scattering on nuclei of the components of the phosphorus acid neutrons having initially energy $E_0 = 2.55$ MeV lose it in conformity with kinematics of the process (Fig. 4). In our case for the particular elements and angles we have the energy of neutrons scattered on O^{16} nuclei 0.90 time less in comparison with the initial one whereas for P^{31} nuclei this figure is 0.95. Then using the well-known formula for the neutrons’ time-of-flight (TOF) method: $E_n(\text{MeV}) = [72.24 l (\text{m}) / t_{\text{TOF}}(\text{ns})]^2$, and taking into consideration TOF of 2.55-MeV neutrons from the source to the bottle axis (3.5 ns), TOF of X-Rays for 2.2 m (7 ns) and delay-time of neutrons’ peak compared to the X-Rays front (6 and 13.5 ns) one may calculate moments of appearance of peak 1 (direct neutrons), peak 2 (neutrons scattered by P^{31} nuclei) and peak 3 (neutrons scattered by O^{16} nuclei). In the above two cases these instants of time should be 96 ns, 101.5 ns, 104.5 ns and 102.5 ns, 109 ns, 112 ns respectively for Fig. 5 (a, b) and Fig. 6 (a, b). Agreement between experiments and calculations looks very good.

However to be sure that these peaks are really belonged to neutrons scattered by nuclei O^{16} and P^{31} , contained in the phosphoric acid, we made an analysis of *relative amplitudes* of these peaks. Cross-sections of elastic scattering of neutrons on these elements in the range 2.45 through 2.7 MeV (i.e. in the range of energies, which corresponds to a change of the angle of the direct neutron beam propagation from the DPF in the relation to its Z-axis) (<http://www.nndc.bnl.gov/exfor/exfor00.htm>) are presented in Fig. 7 (a) and (b) respectively.

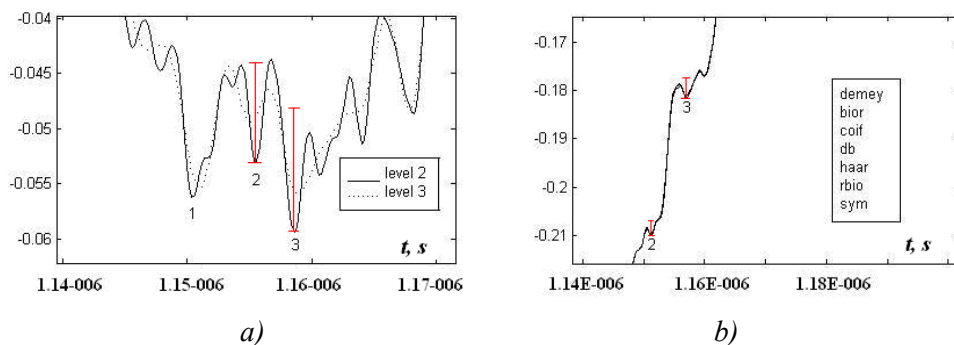


FIG. 6. Oscilloscope traces of FIG. 5 where for de-noising the “dmey” wavelet was used

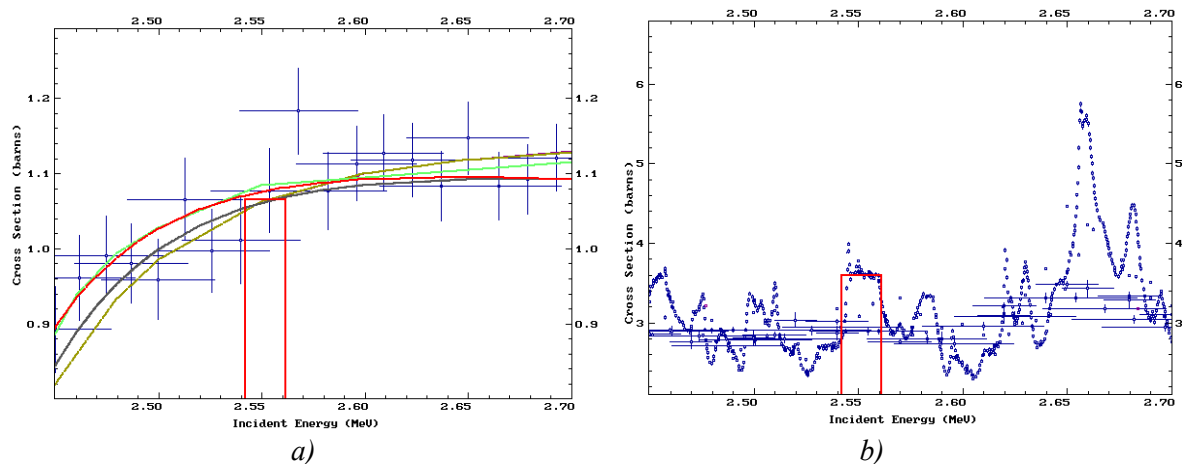


FIG. 7. Cross-sections of elastic neutron scattering by O^{16} (a) and P^{31} (b) nuclei (2.45-2.70 MeV)

In these figures between vertical lines we show a range of neutrons' energy (range of variation of the maximum E_0 of the energy distribution function (EDF) for the beams irradiating our target inside the angle θ). It is clearly seen that for the irradiating beam ($\langle E_0 \rangle = 2.55$ MeV) the value of the cross-section for P^{31} is about 3.3 times higher than it is for the nuclei of O^{16} . But in a molecule of the phosphoric acid the number of oxygen atoms is 4 times higher than that for the phosphorus ones (H_3PO_4). That is why these both peaks are almost equal by their amplitudes (difference is 1.2 times). Of course, to compare these amplitudes one has to subtract background from the overall signal as it is shown by vertical bars in Fig. 6.

NINIS experiment was also performed with the ING-103 device operating with the chamber filled with the D-T mixture as a working gas (14-MeV neutrons, HNO_3 acid). In this case we may expect the following features distinguishing this experiment from previous ones:

1) Utilization of the 14-MeV neutrons will result in a *decrease* of the time-of-flight (TOF) of 14-MeV neutrons – and hence in a corresponding *lower* separation of pulses of *scattered* neutrons from different elements – by a factor of 0.4. It will demand an *increase* in the corresponding TOF base in this case by the 2.5 times, which *decreases* the number of registered scattered neutrons by a factor 6.25. Cross-sections of elastic scattering of neutrons by nuclei of carbon, nitrogen and oxygen (the elements usually presented in explosives) are *less* by 1.5-3 times. However the *neutron yield magnitude* of a DPF *grows* in this case by *one hundred times*. So we shall obtain a *5-10-times benefit* in the scattering signal gain.

2) Neutron energy equal to 14 MeV is well above a number of thresholds of nuclear reactions of neutrons with substances under the interest – oxygen, nitrogen, carbon, hydrogen, etc. Appearance of characteristic γ -rays produced during *an inelastic scattering of 14-MeV neutrons* will provide additional information, which is important for the unveiling procedure.

In Fig. 8 we present results of measurements made with the screen placed in front of the DPF chamber but not blocking scattered neutrons. The screen was the polyethylene/boron bricks of the “Neutronstop” types (attenuation was about 2 orders of magnitude). An analysis of both figures gave us the following information:

- 1) Neutrons scattered by the 1-litre bottle with HNO_3 are clearly seen
- 2) Positions of the neutron pulses in the oscilloscope traces scattered by nitrogen and oxygen nuclei coincide with those calculated for the geometry and distances of our experiment (for PMT+S_1 by 6.0-6.5 ns and for PMT+S_2 by 9.5-10.5 ns later in relation to the peak of direct neutrons correspondingly)

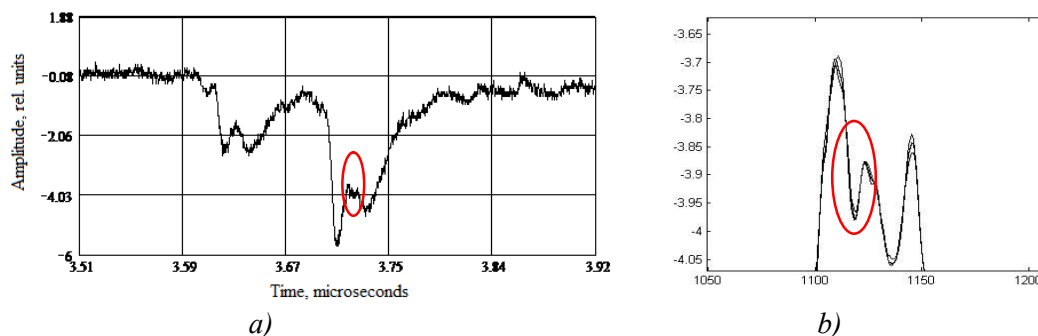


FIG. 8. Input (original) oscilloscope trace at the position of the peak of scattered neutrons (a) and the same trace after wavelet processing on the level 2

3) The distance from the scatterer to the PMT+S_2 chosen for the experiment (544 cm) is not enough for separation of groups of neutrons scattered by nuclei of nitrogen and of oxygen (about 1 ns) for the neutron pulse duration (approximately 20 ns) generated by our DPF chamber in these two shots.

4. Conclusion

Due to these experiments it becomes clear that NINIS technique can be applied in many cases of interrogation of unknown objects, in particular when their size and shape is compared with the space occupied by DPF neutron pulse. Further computer simulations and experiments must be provided for better understanding of limits and restrictions of the method as well as for application of it to interrogation of lengthy objects and fissile materials.

5. Acknowledgements

The authors gratefully acknowledge the support granted to their work by the IAEA (Research Contracts No 14540RO, No 14638RO, and No 14526RO).

Appendix 1: Reference

- [1] CSIKAI, J. "Neutron-based techniques for the detection of concealed objects" (Proc. of the enlargement workshop on "Neutron Measurements and Evaluations for Applications" 5-8 November 2003, Budapest, Hungary), Report EUR 21100 EN
- [2] BROOKS, F.D., et al., "Determination of HCNO concentrations by fast neutron scattering analysis", Nucl. Instr. and Methods in Phys. Res. **A 410** (1998) 319 – 328
- [3] VOURVOPOULOS, G., THORNTON, J., "A Transportable, Neutron-Based Contraband Detection System" (Proc. of Counterdrug Law Enforcement: Applied Technology for Improved Operational Effectiveness), Nashua, NH (1995) 2–39
- [4] GRIBKOV, V.A., MIKLASZEWSKI, R. "On a possibility of the single-shot detection of hidden objects by using nanosecond impulse neutron inspection system", Acta Phys. Chim. Debr. **XXXVIII-XXXIX** (2005) 185-193
- [5] GRIBKOV, V.A., MIKLASZEWSKI, R. "Nanosecond Radiation Pulses for Rapid Detection of Explosives", "Combined Devices for Humanitarian Demining and Explosives Detection" (Proc. IAEA Tech. Meeting, Padova, 2006), IAEA-TM-29225, A-03: http://www-pub.iaea.org/MTCD/publications/PDF/Pub1300_label.pdf